

© Copyright 2008 by the American Chemical Society

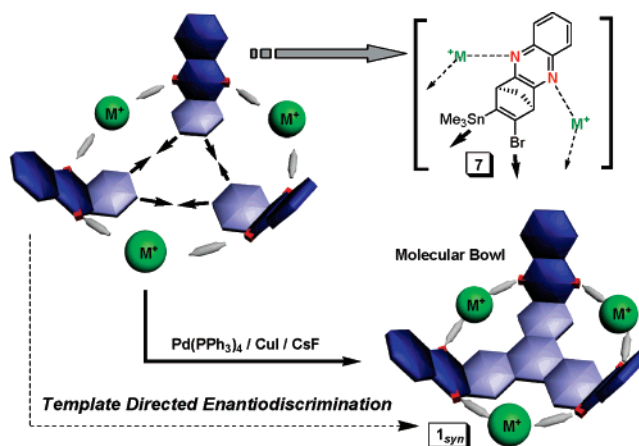
Supramolecular Catalysis at Work: Diastereoselective Synthesis of a Molecular Bowl with Dynamic Inner Space

Zhiqing Yan, Troy McCracken, Shijing Xia, Veselin Maslak, Judith Gallucci,
Christopher M. Hadad, and Jovica D. Badjić*

Department of Chemistry, The Ohio State University, 100 West 18th Avenue, Columbus, Ohio 43210

badjić@chemistry.ohio-state.edu

Received July 16, 2007



The supramolecular assistance to Pd(0)/Cu(I)-catalyzed cyclotrimerization of stannylated norbornene **7** has been investigated to give molecular bowl **1_{syn}** in a stereoselective fashion. Following a divergent strategy, racemic norbornene **7** was synthesized in satisfactory yield. Self-coupling, promoted by Pd(0)/Cu(I) catalysis acting in synergy with CsF, yielded molecular bowl **1_{syn}** in a moderate 30% yield. The reaction diastereoselectivity is affected by the concentration of Cu(I) and Cs⁺: increasing quantities of the cations enhanced the *syn/anti* ratio of the isolated cyclotrimer from statistical (1:3) to a more desirable (4.5:1) ratio, in favor of the molecular bowl **1_{syn}**. ¹H NMR spectroscopic studies suggested the coordinating affinity of **1_{syn}** toward transition metals Cu(I), Ag(I), and Au(I), to account for the observed templation effect. In particular, the tridentate **1_{syn}** has been shown to bind to one Ag(I) cation in the assembly process that is driven with enthalpy ($\Delta H^\circ = -19 \pm 2$ kcal/mol, $\Delta S^\circ = -45$ eu). The complete coordination was not cooperative, and was hypothesized to be impeded with the adverse entropy. Accordingly, density functional theory (BP86) calculations of **1_{syn}** and its mono-, bis-, and tris-Ag(I) complexes suggested that the coordination of one to three silver cations is highly exothermic. The calculations also revealed that the bowl constriction is necessary for the aromatic arms to become preorganized and bind to a silver cation(s) ($\Delta E \approx 8$ kcal/mol). Ultimately, Ag(I) has been shown to assist the diastereoselective formation of **1_{syn}**, lending support to the notion of template-directed synthesis.

Introduction

Broadening the scope and deepening the understanding of molecular recognition and assembly in an unnatural setting requires a steady development of functional hosts capable of binding guests in a constrictive manner.¹ Our research program, focused on the design and study of a family of molecular baskets

and cavitands with controllable conformational dynamics² and regulatory operational mechanisms,³ has the prospect of fundamentally addressing the relationship between recognition and reactivity in artificial environments.⁴ The inspiration comes from

* Address correspondence to this author. Phone: (614) 247-8342. Fax: (614) 292-1685.

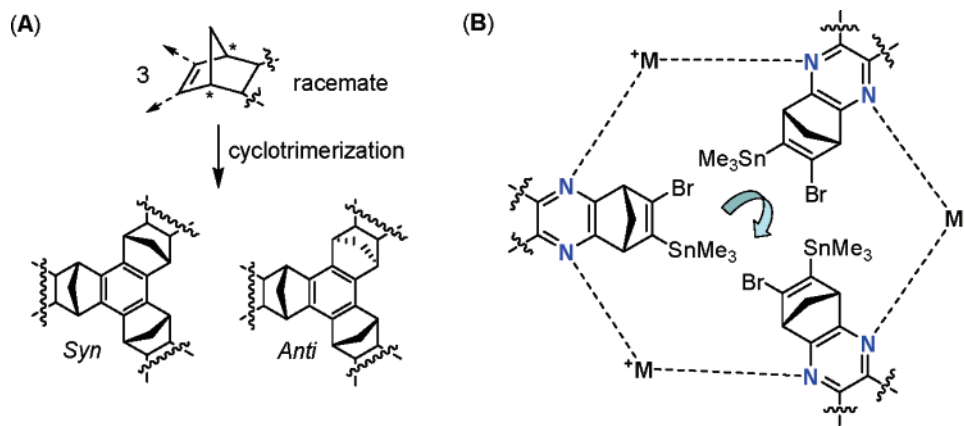


FIGURE 1. (A) The cyclootrimerization of a racemic norbornene, promoted with a transition metal catalyst, typically yields a mixture of *syn/anti* diastereomers; the *anti* compound is statistically favored.^{7,8} (B) Presumably, a metal cation could assist the annulation to occur in a diastereoselective fashion.

the natural world where biological molecules regulate the binding, transition-state stabilization, and trafficking of molecules via a sequence of controlled and synchronized conformational changes.

Molecular baskets, of interest to our program, comprise a C_{3v} symmetrical tris-norbornadiene framework (Figure 1A). The structural framework provides a concave curvature,⁵ and is synthesized via tris-annulation of a functionalized norbornene with a transition metal catalyst.⁶ In general, the reaction gives a *syn/anti* diastereomeric mixture whereby undesired *anti*

compound is typically the principal constituent (Figure 1A).⁷ This statistical challenge limits access to greater quantities of molecular baskets and is frustrating for subsequent molecular recognition studies. A need for a practical diastereoselective cyclootrimerization exists, and De Lucchi et al. have invested considerable effort in developing effective synthetic routes and understanding the annulation mechanisms.^{7,8}

The study presented here communicates an approach, whereby the enantiodiscrimination of a racemic norbornene reactant is assisted with a metal cation as template to direct the formation of a molecular bowl in a diastereoselective fashion (Figure 1B). In addition, the Stille-type cyclootrimerization has, for the first time, been optimized with a palladium(0)/copper(I) catalytic pair to act in synergy with CsF.⁹ Molecular bowl **1_{syn}** (Figure 2A) has been designed in a modular way, and incorporates three identical *o*-phenylenediamine moieties in the quinoxaline form. Conceivably, varying the nature of the diamine component will afford access to a greater number of dynamic receptors and baskets. More spacious inner space of the synthesized molecular bowl is capable of reversibly adjusting its shape and size in response to the presence of silver(I) cations, presenting a stimuli-responsive and dynamic character of this emerging class of hosts.

(1) (a) Judice, J. K.; Cram, D. J. *J. Am. Chem. Soc.* **1991**, *113*, 2790–2791. (b) Quan, M. L. C.; Cram, D. J. *J. Am. Chem. Soc.* **1991**, *113*, 2754–2755. (c) Cram, D. J.; Blanda, M. T.; Paek, K.; Knobler, C. B. *J. Am. Chem. Soc.* **1992**, *114*, 7765–7773. (d) Nakamura, K.; Houk, K. N. *J. Am. Chem. Soc.* **1995**, *117*, 1853–1854. (e) Houk, K. N.; Nakamura, K.; Sheu, C.; Keating, A. E. *Science* **1996**, *273*, 627–629. (f) Sheu, C.; Houk, K. N. *J. Am. Chem. Soc.* **1996**, *118*, 8056–8070. (g) Raymo, F. M.; Houk, K. N.; Stoddart, J. F. *J. Am. Chem. Soc.* **1998**, *120*, 9318–9322. (h) Ihm, C.; Kim, M.; Ihm, H.; Paek, K. *J. Chem. Soc., Perkin Trans. 2* **1999**, *8*, 1569–1575. (i) Chapman, R. G.; Sherman, J. C. *J. Am. Chem. Soc.* **1999**, *121*, 1962–1963. (j) Warmuth, R.; Yoon, J. *Acc. Chem. Res.* **2001**, *34*, 95–105. (k) Yoon, J.; Warmuth, R. *Org. Lett.* **2007**, *9*, 2883–2886.

(2) (a) Maslak, V.; Yan, Z.; Xia, S.; Gallucci, J.; Hadad, C. M.; Badjić, J. D. *J. Am. Chem. Soc.* **2006**, *128*, 5887–5894. (b) Yan, Z.; Xia, S.; Gardlik, M.; Seo, W.; Hadad, C. M.; Badjić, J. D. *Org. Lett.* **2007**, *9*, 2301–2304.

(3) Yan, Z.; Chang, Y.; Mayo, D.; Xia, S.; Maslak, V.; Badjić, J. D. *Org. Lett.* **2006**, *8*, 1697–1700.

(4) (a) Cuevas, F.; Di Stefano, S.; Magrans, J. O.; Prados, P.; Mandolini, L.; de Mendoza, J. *Chem. Eur. J.* **2000**, *6*, 3228–3234. (b) Davis, A. V.; Yeh, R. M.; Raymond, K. N. *Proc. Natl. Acad. Sci. U.S.A.* **2002**, *99*, 4793–4796. (c) Zyryanov, G. V.; Rudkevich, D. M. *Org. Lett.* **2003**, *5*, 1253–1256. (d) Gianneschi, N. C.; Bertin, P. A.; Nguyen SonBinh T.; Mirkin, C. A.; Zakharov, L. N.; Rheingold, A. L. *J. Am. Chem. Soc.* **2003**, *125*, 10508–10509. (e) Fiedler, D.; Bergman, R. G.; Raymond, K. N. *Angew. Chem., Int. Ed.* **2004**, *43*, 6748–6751. (f) Yoshizawa, M.; Miyagi, S.; Kawano, M.; Ishiguro, K.; Fujita, M. *J. Am. Chem. Soc.* **2004**, *126*, 9172–9173. (g) Palmer, L. C.; Rebek, J., Jr. *Org. Biomol. Chem.* **2004**, *2*, 3051–3059. (h) Kaanumalle, L. S.; Gibb, C. L. D.; Gibb Bruce, C.; Ramamurthy, V. *J. Am. Chem. Soc.* **2004**, *126*, 14366–14367. (i) Hooley, R. J.; Rebek, J., Jr. *J. Am. Chem. Soc.* **2005**, *127*, 11904–11905. (j) Luetzen, A. *Angew. Chem., Int. Ed.* **2005**, *44*, 1000–1002. (k) Lagona, J.; Mukhopadhyay, P.; Chakrabarti, S.; Isaacs, L. *Angew. Chem., Int. Ed.* **2005**, *44*, 4844–4870. (l) Yoshizawa, M.; Tamura, M.; Fujita, M. *Science* **2006**, *312*, 251–254.

(5) (a) Siegel, J. *Angew. Chem., Int. Ed. Engl.* **1994**, *33*, 1721–1723. (b) Frank, N. L.; Baldrige, K. K.; Gantzel, P.; Siegel, J. S. *Tetrahedron Lett.* **1995**, *36*, 4389–4392. (c) Buergi, H.-B.; Baldrige, K. K.; Hardcastle, K.; Frank, N. L.; Gantzel, P.; Siegel, J. S.; Ziller, J. *Angew. Chem., Int. Ed. Engl.* **1995**, *34*, 1454–1456.

(6) (a) Gassman, P. G.; Gennick, I. *J. Am. Chem. Soc.* **1980**, *102*, 6863–6864. (b) Durr, R.; De Lucchi, O.; Cossu, S.; Lucchini, V. *Chem. Commun.* **1996**, *2*, 2447–2448. (c) Durr, R.; Cossu, S.; Lucchini, V.; De Lucchi, O. *Angew. Chem., Int. Ed. Engl.* **1997**, *36*, 2805–2807. (d) Sakurai, H.; Daiko, T.; Hirao, T. *Science* **2003**, *301*, 1878–1882.

(7) (a) Zonta, C.; Cossu, S.; Peluso, P.; De Lucchi, O. *Tetrahedron Lett.* **1999**, *40*, 8185–8188. (b) Cossu, S.; De Lucchi, O.; Paulon, A.; Peluso, P.; Zonta, C. *Tetrahedron Lett.* **2001**, *42*, 3515–3518. (c) Peluso, P.; De Lucchi, O.; Cossu, S. *Eur. J. Org. Chem.* **2002**, *23*, 4032–4036.

(8) (a) Fabris, F.; De Martin, A.; De Lucchi, O. *Tetrahedron Lett.* **1999**, *40*, 9121–9124. (b) Paulon, A.; Cossu, S.; De Lucchi, O.; Zonta, C. *Chem. Commun.* **2000**, *19*, 1837–1838. (c) Cossu, S.; Cimentini, C.; Peluso, P.; Paulon, A.; De Lucchi, O. *Angew. Chem., Int. Ed.* **2001**, *40*, 4086–4089. (d) Borsato, G.; De Lucchi, O.; Fabris, F.; Groppo, L.; Lucchini, V.; Zambon, A. *J. Org. Chem.* **2002**, *67*, 7894–7897. (e) Borsato, G.; De Lucchi, O.; Fabris, F.; Lucchini, V.; Pasqualotti, M.; Zambon, A. *Tetrahedron Lett.* **2002**, *44*, 561–563. (f) Fabris, F.; Bellotto, L.; De Lucchi, O. *Tetrahedron Lett.* **2003**, *44*, 1211–1213. (g) Zonta, C.; Fabris, F.; De Lucchi, O. *Org. Lett.* **2005**, *7*, 1003–1006.

(9) (a) Liebeskind, L. S.; Fengi, R. W. *J. Org. Chem.* **1990**, *55*, 5359–5364. (b) Han, X.; Stolz, B. M.; Corey, E. J. *J. Am. Chem. Soc.* **1999**, *121*, 7600–7605. (c) Casado, A. L.; Espinet, P. *Organometallics* **2003**, *22*, 1305–1309. (d) Mee, S. P. H.; Lee, V.; Baldwin, J. E. *Angew. Chem., Int. Ed.* **2004**, *43*, 1132–1136.

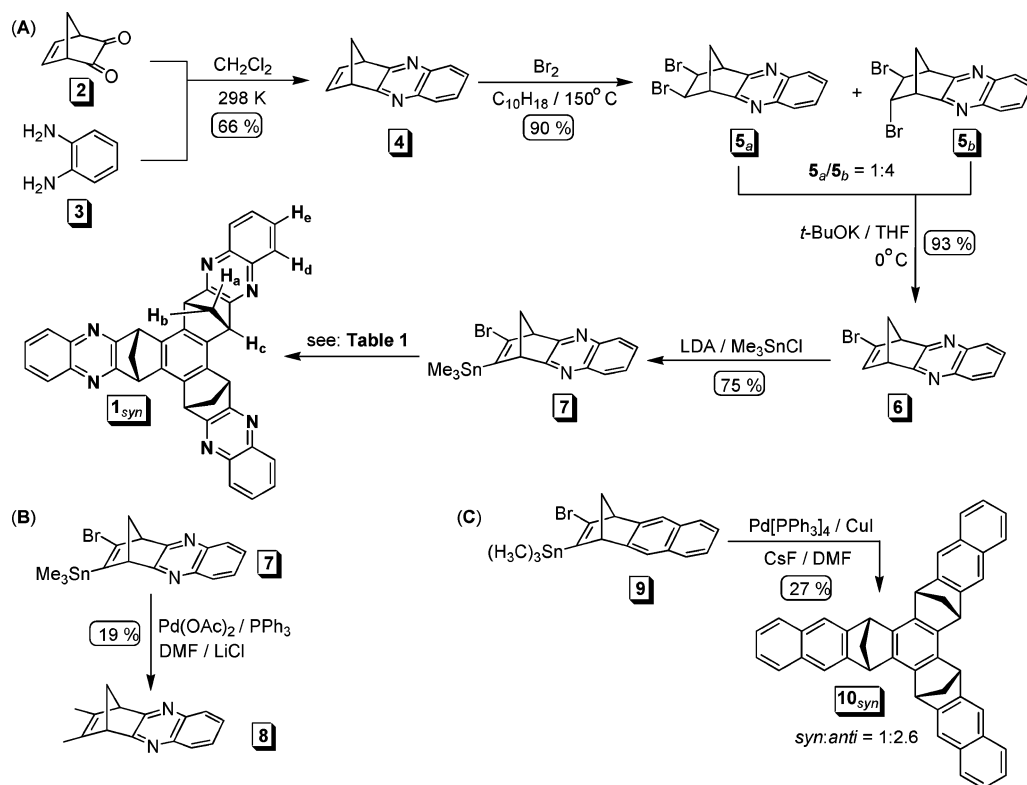


FIGURE 2. (A) Synthesis of compound **1_{syn}** and its ¹H NMR spectroscopic assignment. (B) Synthesis of compound **8**. (C) Synthesis of compound **10**.

Results and Discussion

Synthesis. The synthesis of **1_{syn}** is presented in Figure 2A. Compounds **2** and **3** were obtained independently, and then subjected to condensation to give **4**. The strategy is divergent to allow for a number of accessible diamines, akin to 1,2-diaminobenzene **3**, to be ultimately used in the synthesis; in this way, the versatility of the procedure is greatly enhanced. Furthermore, 5-norbornene-2,3-dione **2** is easily obtained in gram quantities from a Diels–Alder reaction of vinylene carbonate¹⁰ and cyclopentadiene followed by the hydrolysis and Swern oxidation of subsequently formed cycloadduct.¹¹ The bromination of **4** was completed in boiling decalin at 150 °C to circumvent Wagner–Meerwein skeletal rearrangements (Figure 2A).¹² Both *cis* and *trans* addition of bromine took place, with the stereochemistry of the *cis* addition preferring the *exo* side of the bicyclic ring.¹³ Subsequent elimination of the halogen in **5_{a/b}**, assisted with *t*-BuOK, and stannylation afforded bromo(trimethylstannyl) **7**. This compound is preset to undergo the cyclotrimerization, when prompted with a transition metal catalyst.

Cyclotrimerization Studies. Modularly designed **7** has two aromatic nitrogens with an intrinsic ability to complex transition metals, perhaps, in the course of its coupling into **1** (Figure 1B). That is to say, a metal cation can be hypothesized to act

as a template¹⁴ in the formation of the cyclotrimer: the process of enantiomeric discrimination, in the course of homocoupling versus heterocoupling of racemic **7**, may well be assisted with the template to favor the *syn* product.

With this presumption, we first attempted the cyclotrimerization of **7** using Cu(I) and Cu(II) compounds to catalyze and simultaneously template the formation of desired **1_{syn}** (Table 1, entries 1–3). Copper-based reagents proved ineffective in promoting the transformation: a mixture of unidentifiable oligomers and destannylated products was typically observed. It is important to note, though, that the cyclotrimerization of a variety of stannylated norbornenes assisted with copper catalysts had, as reported earlier,^{6c,7a,8d} been proven useful. The self-coupling of **7**, under the Stille conditions, also failed to give the desired product.^{8b} It surprisingly, led to a transfer of two methyl groups to the trigonal carbons in **7** to give **8** in 19% yield (Figure 1B). The X-ray structural analysis confirmed the identity of this compound.¹⁵ The transfer of an alkyl group to a trigonal carbon is typically a slow process.¹⁶ It is the sole reason for the widespread use of trialkyltin derivatives in Stille couplings, with alkyl groups as “nontransferable” ligands. Herein observed simultaneous formation of two carbon–carbon bonds

(10) Newman, M. S.; Addor, R. W. *J. Am. Chem. Soc.* **1955**, *77*, 3789–3793.

(11) Kobayashi, T.; Kobayashi, S. *Molecules* **2000**, *5*, 1062–1067.

(12) (a) Colter, A.; Friedrich, E. C.; Holness, N. J.; Winstein, S. *J. Am. Chem. Soc.* **1965**, *87*, 378–379. (b) Walling, C. *Acc. Chem. Res.* **1983**, *16*, 448–454. (c) Tutar, A.; Taskesenligil, Y.; Cakmak, O.; Abbasoglu, R.; Balci, M. *J. Org. Chem.* **1996**, *61*, 8297–8300.

(13) Kobayashi, T.; Miki, K. *Bull. Chem. Soc. Jpn.* **1998**, *71*, 1443–1449.

(14) For recent reviews explaining the principles of template-directed synthesis see: (a) Jager, R.; Vogtle, F. *Angew. Chem., Int. Ed. Engl.* **1997**, *36*, 930–944. (b) Hubin, T. J.; Kolchinski, A. G.; Vance, A. L.; Busch, D. H. *Adv. Supramol. Chem.* **1999**, *5*, 237–357. (c) Arico, F.; Badjić, J. D.; Flood, A.; Leung, K.; Liu, Y.; Stoddart, J. F. *Top. Curr. Chem.* **2005**, *249*, 203–261. (d) Lankshear, M. D.; Beer, P. D. *Coord. Chem. Rev.* **2006**, *250*, 3142–3160.

(15) See the Supporting Information for more details.

(16) (a) Stille, J. K. *Angew. Chem., Int. Ed. Engl.* **1986**, *25*, 508. (b) Farina, V.; Krishnamurthy, V.; Scott, W. J. *Organic Reactions*; Paquette, L. A., Ed.; John Wiley & Sons, Inc.: New York, 1997; Vol. 50. (c) Espinet, P.; Echavarren, A. M. *Angew. Chem., Int. Ed.* **2004**, *43*, 4704–4734.

TABLE 1. The Cyclotrimerization of **7** into **1_{syn}** Was Conducted under Modified Stillé Conditions and Assisted with Cu(I), Cs⁺, and Ag(I) Cations in a Template-Directed Fashion

entry	Pd catalyst	Cu salt (%) ^a	inorganic component (molar equiv) ^a	overall yield of 1 , ^b %	<i>syn/anti</i> 1
1		CuTc		0	
2		CuI	LiCl	0	
3		Cu(NO ₃) ₂		0	
4	Pd(OAc) ₂		LiCl	0	
5	Pd(PPh ₃) ₄	CuI (0)	CsF (2.0)	0	
6	PdCl ₂	CuI (4)	CsF (2.0)	24	1:3
7	PdCl ₂	CuI (20)	CsF (2.0)	29	1:1.4
8	Pd(PPh ₃) ₄	CuI (20)	CsF (2.0)	35	1.3:1
9	Pd(PPh ₃) ₄	CuI (70)	CsF (2.0)	23	2.3:1
10	Pd(PPh ₃) ₄	CuI (20)	TBAF (2.0)	0	
11	Pd(PPh ₃) ₄	CuI (20)	NaF (2.0)	0	
12	Pd(PPh ₃) ₄	CuI (20)	CsF (1.0)	23	1.5:1
13	Pd(PPh ₃) ₄	CuI (20)	CsF (2.0)	24	4.5:1
			CsClO ₄ (8.0)		
14	Pd(PPh ₃) ₄	CuI (20)	CsF (2.0)	20	4.4:1
			AgOTf (2.0)		

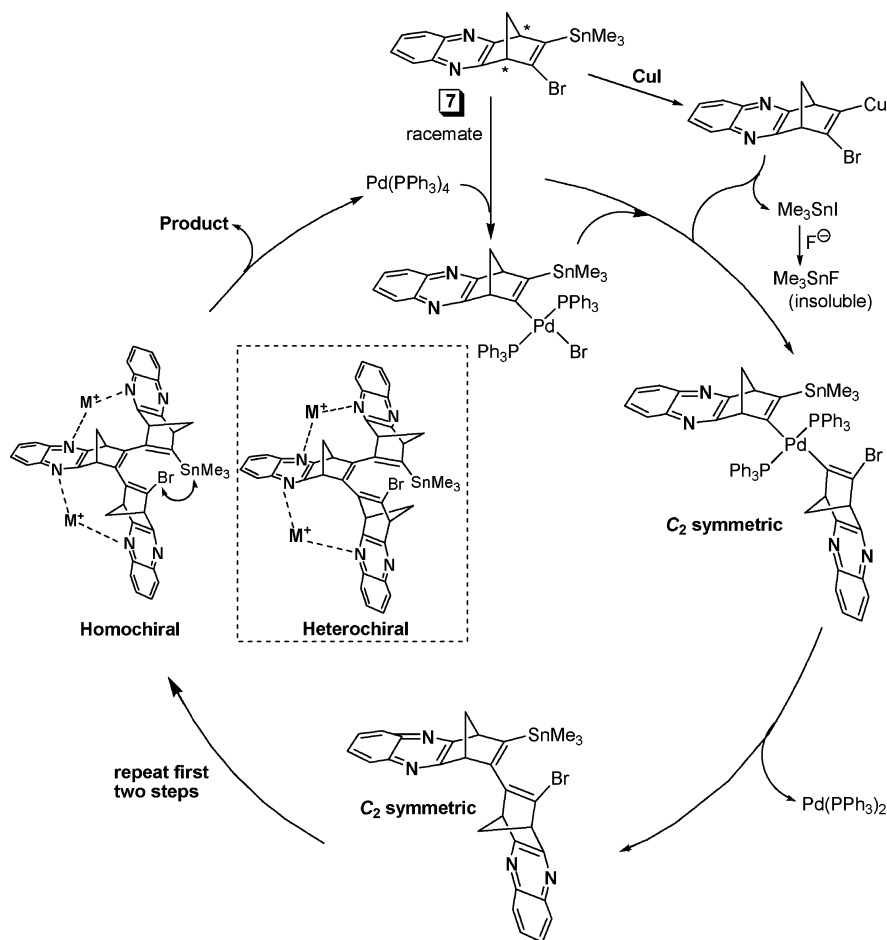
^a With respect to the quantity of **7**. ^b Isolated yield.

(Figure 1B) is unique,¹⁵ and likely facilitated by a slow transmetalation step whereby the transfer of an electron-deficient vinyl group is retarded in a sterically congested chemical environment. In a Heck-type promoted self-coupling of **6** to give **1** (Table 1; entry 4), the starting material was only partially recovered.^{7b}

Baldwin et al. have recently revealed a synergistic effect of Cu(I) salts and fluoride anion in the Stillé coupling of electron-deficient stannanes with vinyl/aryl halides and triflates.^{9c} When

the procedure was applied in the cyclotrimerization of **7**, compound **1** was obtained as a mixture of the *syn/anti* isomers in a moderate yield (Table 1; entries 6–9). The reaction diastereoselectivity has, intriguingly, been found to be a function of the amount of Cu(I): (a) in the absence of copper, there was no reaction (Table 1; entry 5), (b) low amounts of copper (4%) led to a 1:3 statistical *syn/anti* ratio of the diastereomers (Table 1, entry 6), and (c) higher concentrations of Cu(I) (20–70%) afforded **1_{syn}** as the major product (Table 1; entries 7–9). It is

SCHEME 1. A Proposed Mechanism for the Cyclotrimerization of Racemic **7**



generally believed that Cu(I) accelerates the Stille coupling via enhancing the transmetalation step whereby a more reactive organocopper intermediate is formed from the organostannane (Scheme 1).^{9a,b} The present case, evidently, implicates an additional Cu(I) role in the catalytic cycle: the cation perhaps augments the reaction diastereoselectivity via templation (Figure 1B and Scheme 1). Alternatively, F⁻ has been hypothesized to contribute in removing tin salts from the catalytic equilibrium, which in turn supports the formation of more reactive organocopper intermediate so that the reaction becomes accelerated (Scheme 1).^{9c} In the trimerization of **7**, the nature of the fluoride counterbalancing cation has been revealed to be critical: cesium, but not Bu₄N⁺ or Na⁺, supported the formation of **1** (Table 1, entries 10–13). Even more, the increased presence of the large and soft Cs⁺ cation (from 1.0 to 10.0 molar equiv) enhanced the reaction diastereoselectivity practically by a factor of 3 (Table 1, entries 12 and 13). Evidently, Cs⁺ and Cu(I) cations work in synergy and their mutual presence is necessary for converting **7** into **1**.

In a control experiment, we conducted the cyclotrimerization of naphthobenzonorbomadiene derivative **9**, lacking the aromatic nitrogens (Figure 2C). Almost a statistical *syn/anti* ratio (1:2.6) of the isolated cyclotrimer **10** was obtained, further supporting the notion of template-directed formation of **1_{syn}**.

Catalytic Mechanism. A tentative mechanism for the chain-type conversion (Figure 1B) of **7** to **1** is summarized in Scheme 1. Supposedly, Cu(I) and Cs⁺ cations promote homo- over heterochiral coupling of racemic **7**. That is to say, in case of homochiral C₂ symmetrical intermediates and **1_{syn}**, the coordination of the cations to the aromatic nitrogens can be hypothesized to assist their formation and the subsequent cross-coupling. The coordination, in particular, can preorganize the homochiral intermediate containing three norbornenes to the extent that the activation energy for the benzene ring annulation is minimized (Scheme 1). In fact the analogous C_s symmetrical intermediates (only one shown in Scheme 1) must be twisted upon complexing the metal cations. The twisted and “out-of-plane” geometry would disfavor the transmetalation and the overall intramolecular coupling providing a mechanism for the oligomerization.

It is interesting to note that the increasing amounts of the *syn* isomer, produced in the catalysis, suppressed the formation of the *anti* diastereomer (Table 1; entries 6–9, 12, and 13). In that respect, the overall reaction yields, for all transformations, were rather low and comparable (20–35%). One could anticipate that the enhanced formation of the *syn* isomer, promoted with the “correct” metal cation, would also be accompanied by the increased overall reaction yield. Apparently, the undesired “side” reactions (possible oligomerizations and such) are kinetically favored to a great extent. The presence of the templating metal cations evidently upsets the kinetics of the *syn/anti* formation, yet making the cyclotrimerization still not competitive to the fast formation of the side product(s).

¹H NMR Spectroscopic Studies. To examine the complexation affinity of different metals toward molecular bowl **1_{syn}** and to gain more insight into the templation mechanism, we originally conducted a series of ¹H NMR spectroscopic titrations (Figures 3 and 4). A gradual addition of cesium salt (CsPF₆) to a solution of **1_{syn}** (3.5 mM, CD₃CN) caused minor changes in its ¹H NMR spectrum (Figure 3b).¹⁶ In contrast, when [Cu(CH₃CN)₄]PF₆, AgOTf, or [Au(PPh₃)₃]Cl were individually titrated to a solution of **1_{syn}** (Figure 3c–e), the ¹H NMR signals were affected: Cu(I) imposed the least change, while Ag(I)

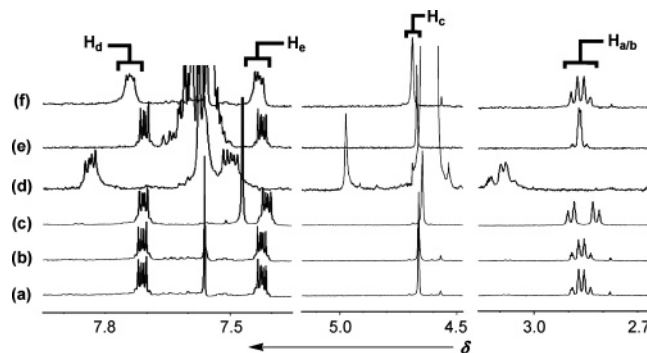


FIGURE 3. A series of ¹H NMR (500 MHz, 298 K) spectra of the following: (a) **1_{syn}** (9.4 mM, CD₃CN/CDCl₃, 5:1), (b) **1_{syn}** (9.4 mM, CD₃CN/CDCl₃, 5:1) and 3.3 mol equiv of CsPF₆, (c) **1_{syn}** (9.4 mM, CD₃CN/CDCl₃, 1:1) and 4.4 mol equiv of [Cu(I)(CH₃CN)₄]PF₆, (d) **1_{syn}** (2.3 mM, CD₃OD/CDCl₃, 1:1) and 4.8 mol equiv of AgOTf, (e) **1_{syn}** (5.9 mM, CD₃CN) and 6.2 mol equiv of [Au(I)PPh₃]Cl, and (f) **1_{syn}** (9.4 mM, CD₃CN/CDCl₃, 5:1) and 3.3 mol equiv of CsPF₆ and 24 mol equiv of [Cu(I)(CH₃CN)₄]PF₆.¹⁶ For the ¹H NMR spectroscopic assignment of **1_{syn}**, see Figure 2A.

created the greatest perturbations in the NMR signals.¹⁶ In a control experiment,¹⁶ AgOTf was added to a solution of molecular bowl **10_{syn/anti}**,¹⁶ lacking the aromatic nitrogens. The absence of any detectable spectroscopic changes for **10_{syn}** is consistent with the notion that the heterocyclic arms are critical for coordinating to the transition metal cation.¹⁶

In the titration experiment with a standard solution of AgOTf (0.168 M, CD₃OD/CDCl₃ = 1:1), the ¹H NMR signals of **1_{syn}** (2.3 mM, CD₃OD/CDCl₃ = 1:1) shifted downfield as the concentration of Ag(I) was gradually increased (Figure 4A). The break in the titration curve at 1.0 mM concentration of the metal cation (Figure 4B) points to 1:1 binding stoichiometry;¹⁷ indeed, the method of continuous variation (Job plot) confirmed this stoichiometric ratio.^{16,18} In addition, a MALDI-TOF mass spectrometric measurement of a solution of **1_{syn}** and AgOTf also suggest the existence of the [**1_{syn}**:Ag]⁺ complex as the major component of the mixture.¹⁶ The nonlinear curve fitting of the binding isotherm (Figure 4B) to a 1:1 equilibrium binding model yielded an apparent association constant of $K_{\text{avg}} = (5.6 \pm 1.6) \times 10^3 \text{ M}^{-1}$.^{16,17} The observed low-field ¹H NMR chemical shifts of the signals in **1_{syn}** (Figure 4A), upon addition of Ag(I), are consistent with the coordination of a positively charged Ag(I) to two adjacent aromatic heterocyclic rings in **1_{syn}**: the coordination reorganizes the electron density making the proton nuclei magnetically deshielded. Interestingly, the signals for the bridge H_a/H_b protons experienced a considerable change ($\Delta\delta = 0.22$), despite their angular position that depresses through-bond communication with the aromatic appendages.¹⁹ To accommodate a silver cation, the aromatic arms in **1_{syn}** have to fold inside (Figure 6B) causing the bridge carbon and its protons to move away from the center of the arms. With such conformational changes, the diamagnetic effect imposed on the

(17) Wilcox, C. *Frontiers in Supramolecular Organic Chemistry and Photochemistry*; Schneider, H.-J., Durr, H., Eds.; Wiley-VCH: Weinheim, Germany, 1991; pp 123–143.

(18) (a) Connors, K. A. *Binding Constants, The Measurement of Molecular Complex Stability*; Wiley-Interscience: New York, 1987; pp 24–28. (b) Blanda, M. T.; Horner, J. H.; Newcomb, M. J. *Org. Chem.* **1989**, *54*, 4626–4636.

(19) (a) Wilcox, C. F.; Leung, C. J. *J. Am. Chem. Soc.* **1968**, *90*, 336–341. (b) Cole, T. W., Jr.; Mayers, C. J.; Stock, L. M. *J. Am. Chem. Soc.* **1974**, *96*, 4555–4557. (c) Grubbs, E. J.; Wang, C.; Deardurff, L. A. *J. Org. Chem.* **1984**, *49*, 4080–4082.

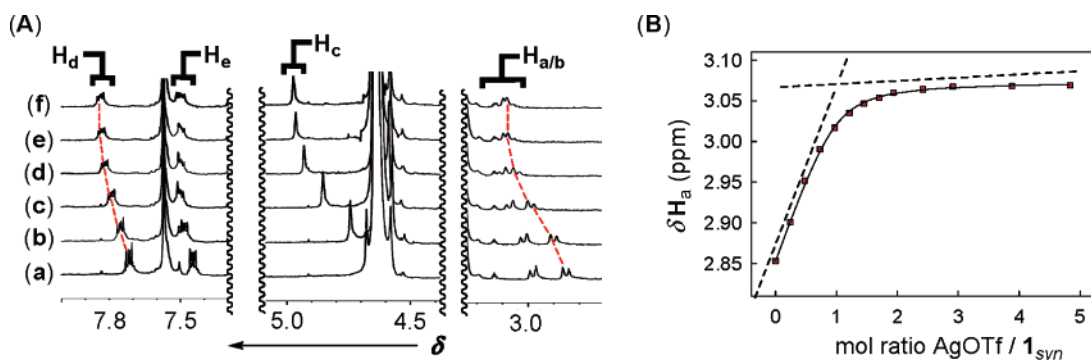


FIGURE 4. (A) A series of ^1H NMR spectra (500 MHz, 298 K, $\text{CD}_3\text{OD}/\text{CDCl}_3$, 1:1) of $\mathbf{1}_{\text{syn}}$ (2.3 mM) recorded on gradual addition of 0.168 M standard solution of AgOTf ($\text{CD}_3\text{OD}/\text{CDCl}_3$, 1:1) such that the final mixture comprises (a) 0, (b) 0.24, (c) 0.73, (d) 1.45, (e) 2.91, and (f) 4.84 mol equiv of AgOTf. (B) The nonlinear curve fitting of the ^1H NMR chemical shifts of the H_a resonance in $\mathbf{1}_{\text{syn}}$ to a 1:1 equilibrium model.^{22,23}

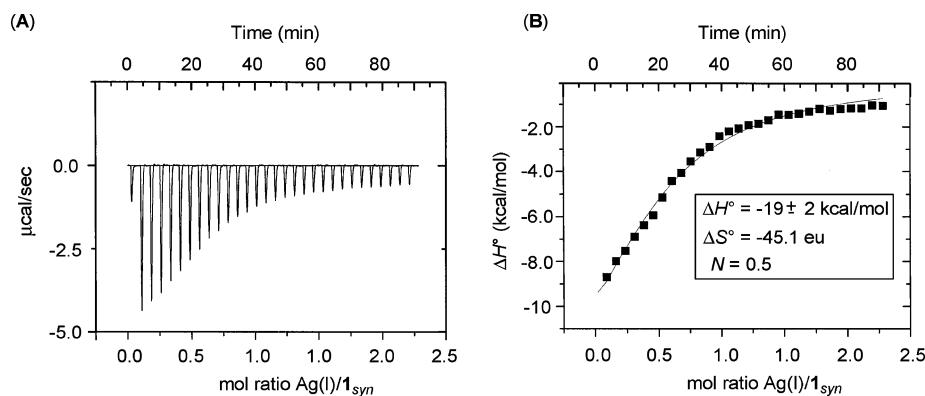


FIGURE 5. (a) Isothermal titration calorimetry (ITC) data for the titration of a solution of $\mathbf{1}_{\text{syn}}$ (0.173 mM, 1.40 mL) with a 1.75 mM standard solution of AgOTf ($\text{CHCl}_3/\text{CH}_3\text{OH} = 1:1$) at 300 K. (b) Computer simulated curve fitting afforded the thermodynamic parameters for the assembly.

$\text{H}_{a/b}$ protons becomes less pronounced, which, we reason, then rendered the observed downfield changes. The host–guest exchange, and the Ag(I) revolving about $\mathbf{1}_{\text{syn}}$, must be rapid on the NMR time scale, to explain the observed proton signals corresponding to an averaged C_{3v} symmetrical species (Figure 4A).

Isothermal Titration Calorimetry (ITC). The thermodynamic profile for the binding of Ag(I) to $\mathbf{1}_{\text{syn}}$ was further investigated with isothermal titration calorimetry (Figure 5). A standard solution of AgOTf (1.75 mM, $\text{CH}_3\text{OH}/\text{CHCl}_3$, 1:1) was successively added to a solution of host $\mathbf{1}_{\text{syn}}$ (0.173 mM, $\text{CH}_3\text{OH}/\text{CHCl}_3$, 1:1), contained in the sample cell. The total heat released in the interaction (ΔH°) was measured to give the binding isotherm (Figure 5A). The experiments showed that the assembly is exothermic ($\Delta H^\circ = -19 \pm 2$ kcal/mol). The fitting to the one-site model revealed $K_a = (1.4 \pm 0.2) \times 10^4 \text{ M}^{-1}$ ($\Delta G^\circ = -5.7 \pm 0.5$ kcal/mol, 300.0 K) and $N = 0.5$ as independent fit parameters. The association constant is, apparently, in fair agreement with the one obtained from the ^1H NMR titration (Figure 4B). The observed binding stoichiometry (N) is noticeably off the scale. Supposedly, the existence of two other thermodynamic states, in which Ag(I) is coordinated to the second and third binding site in $\mathbf{1}_{\text{syn}}$, can in part be accounted for the apparent “deviations” in the theoretical isotherm (Figure 5b) and the off-scale stoichiometry. The self-association of $\mathbf{1}_{\text{syn}}$ in solution can also contribute to the effect (see the paragraph about the X-ray diffraction studies and Figure 7B). The formation of single complexed $\mathbf{1}_{\text{syn}}$ is to a large extent hampered by entropy (Figure 5, $\Delta S^\circ = -45$ eu). This loss of entropy can, to a first approximation, be ascribed to the rigidity of the formed

host–guest complex ($\Delta H^\circ = -19 \pm 2$ kcal/mol), and the enthalpy/entropy compensation effect.²⁰ The solvent reorganization must also contribute, although in a more complicated fashion.

Theoretical Calculations. Density functional theory (DFT, BP86 functional) calculations²¹ of the optimized geometry of $\mathbf{1}_{\text{syn}}$ and its corresponding complex with a Ag(I) cation [$\mathbf{1}_{\text{syn}}:\text{Ag}$]⁺ suggested a high thermodynamic stability of the complex ($\Delta E = -9.0$ kcal/mol, Figure 6B). For the coordination to take place, two aromatic arms in $\mathbf{1}_{\text{syn}}$ need to move toward the inner space to bring the aromatic nitrogens to the proper distance ($\Delta D = 1.0$ Å). The conformational change is accompanied by the decrease in the dihedral angle ($\Delta\alpha = 2.0^\circ$) and relocation of the bridge protons somewhat away from the neighboring quinoxaline aromatic rings (Figure 6B); the calculation is indeed in agreement with the observed ^1H NMR chemical changes for $\text{H}_{a/b}$ protons (Figure 4). *What does prevent three silver cations from cooperatively coordinating to the nitrogen ligands of the bowl and thus causing its complete folding?*

To address this matter, the synchronized inward/outward motion of the arms in the bowl itself has been subjected to a series of DFT calculations whereby each energy minimization had the distance between the aromatic nitrogens constrained, with all other parameters being fully optimized (Figure 6A). The calculated potential energy profile for the bowl “swinging” turned out to be asymmetric: the bowl constriction about the

(20) Ruloff, R.; Seelbach, U. T.; Merbach, A. E.; Klärner, F.-G. *J. Phys. Org. Chem.* **2002**, *15*, 189–196.

(21) (a) Perdew, J. P. *Phys. Rev. B* **1986**, *33*, 8822. (b) Becke, A. D. *Phys. Rev. A* **1998**, *38*, 3098.

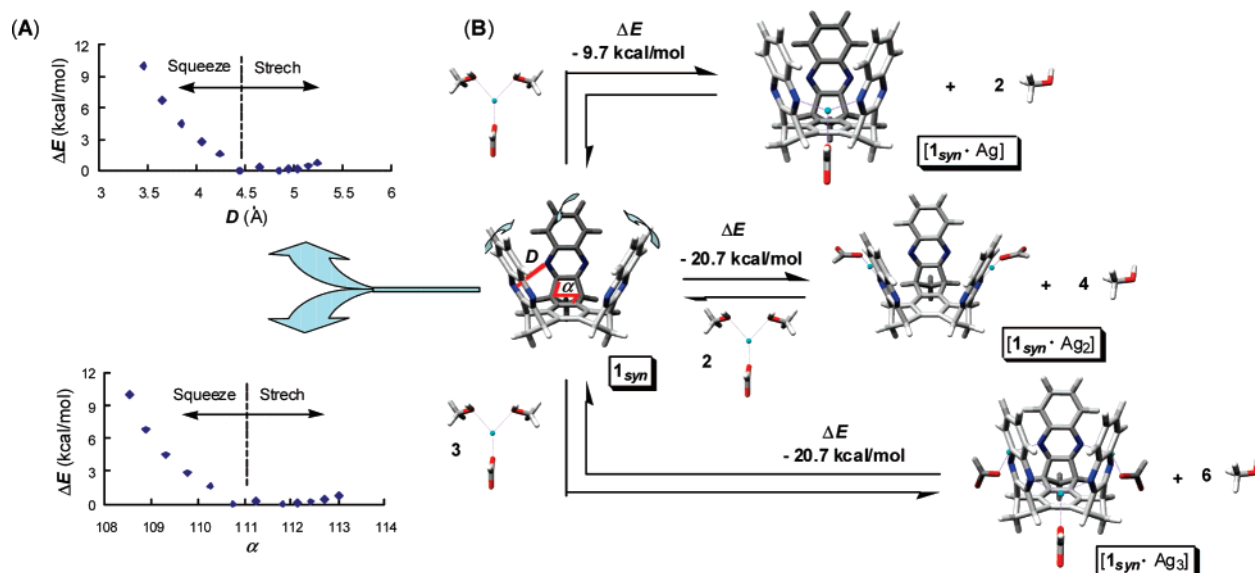


FIGURE 6. Energy minimized (DFT, BP86) conformation of 1_{syn} , and calculated potential energy diagrams for the synchronized inward/outward motion of its arms as a function of the dihedral angle α and the distance between the adjacent nitrogens D . (B) Energy minimized structures (BP86) of mono-, bis-, and tris-coordination complexes of 1_{syn} with Ag(I).

energy well is endothermic, while the energy required to open is more neutral (Figure 6A). The energy required to constrict the dihedral angles ($\Delta\alpha = 3.5^\circ$) and at the same time dislocate the aromatic nitrogens ($\Delta D = 1.08 \text{ \AA}$) in 1_{syn} , to preorganize the molecule for coordination to three Ag(I) cations is high ($\Delta E > 8$ kcal/mol, Figure 6A). The formation of three Ag–N coordinative bonds, based on these calculations, should, however, be sufficiently exothermic to make the overall complexation thermodynamically favorable (at least -20.7 kcal/mol, Figure 6B). On the other hand, the great entropic cost that accompanies the binding of the first Ag(I) to 1_{syn} ($\Delta S^\circ_{(expt)} = -45$ eu, Figure 5B) is likely to propagate to the second and third coordination, making the overall interaction thermodynamically unfeasible.

Thermodynamic Considerations and Rational Summation of the Supramolecular Assistance to Catalysis. The observed low propensity of Cu(I) and Au(I) to coordinatively bridge the arms in 1_{syn} (Figure 3) can now be ascribed to the copper size and the gold complexing character. In particular, the coordination of small Cu(I) and soft Au(I) cations can be hypothesized to provide insufficient enthalpic driving force, which is necessary to surmount the energy required for the bowl to acquire its optimal binding geometry; the entropy effect needs to be taken into account, as well. In the case of copper, however, its interaction with 1_{syn} and other intermediates in the course of the cyclotrimerization (Scheme 1) is strong enough to provide sufficient transition-state stabilization to boost the reaction diastereoselectivity.

The coordinating affinity of Cu(I) toward 1_{syn} , with and without cesium cation present in solution, is practically indistinguishable (Figure 2c/f).¹⁶ Intriguingly, DFT calculations (BP86) of energy minimized $[1_{syn}:\text{Cu}(\text{I})_3]^{3+}[\text{CsF}]$ suggest the binding mode in which cesium facilitates the bowl constriction via its cation– π interaction with the aromatic arms at the top rim (Figure 7A), thereby shortening the N...N distance between adjacent arms of the bowl.¹⁶ The energy minimization of $[1_{syn}:\text{Cu}(\text{I})_3]\text{Cl}_3$, without cesium present, was proven to be problematic, and did not undergo the expected convergence at the BP86

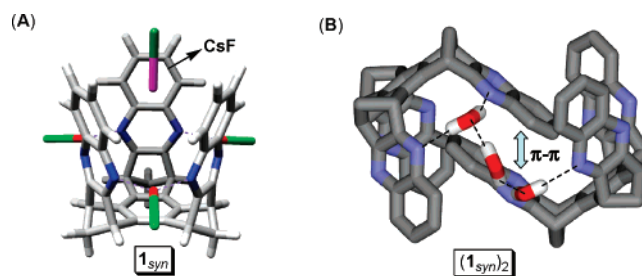


FIGURE 7. (A) Energy minimized (DFT, BP86) conformation of 1_{syn} coordinated to three Cu(I) cations and containing CsF at its top rim. (B) Stick representation of the structure of the 1_{syn} dimer in the solid state (hydrogen atoms are omitted for clarity).

level. The observed synergistic action of two cations, Cu(I) and Cs^+ , in the templating of 1_{syn} can thus, to an extent, be rationalized.

In consideration of the Ag(I) aptitude toward coordinating 1_{syn} , it is conceivable to presume for this cation to template the formation of the bowl as well. Indeed, when AgOTf (2.0 mol equiv) was used in the cyclotrimerization of **7**, under the standard conditions, 1_{syn} was obtained in excess (Table 1, entry 14).²² The reaction diastereoselectivity, in favor of the *syn* isomer (4.4:1), lends support to the notion of a template-directed mechanism (Scheme 1).

X-Ray Diffraction Studies. A single-crystal X-ray study of 1_{syn} revealed a repeating motif comprised of two fully entangled molecular bowls, bridged with three molecules of water (Figure 7B).²³ Each bowl places an arm in the cavity of its partner at the π – π stacking distance (3.5 Å). Notably, the π -deficient portion of one arm is against the π -rich portion of another. The directional assembly in the solid state is thus in accord with the electrostatic Hunter–Sanders model for aromatic interactions.³¹ Furthermore, the observed ordering allows the bowl to fill its inner space in the entropically most efficient manner,

(22) For an additional role of Ag(I) in improving Stille couplings see: Gronowitz, S.; Messmer, A.; Timari, G. *J. Heterocycl. Chem.* **1992**, *29*, 1049–.

i.e., by excluding the solvent molecules as potential external guests. The calculated bowl interior volume can be approximated to 205 Å.³² When positioned inside of **1_{syn}**, a partially incorporated quinoxaline arm (108.7 Å³) occupies 53% of the available space, which is interestingly proportionate to packing coefficients (PC) of liquids.³² This analysis needs to be taken with some caution, as it is difficult to obtain the accurate inner volume of **1_{syn}**: the molecule encompasses three sizable side portals and a large opening at the rim. Three water molecules are organized such that two share both of their hydrogen atoms with quinoxaline nitrogens of the entangled bowls (Figure 7B). The remaining one serves as a hydrogen-bonding linker in between them. On the basis of the experimental N—H···N (2.9 Å) and O—H···O (2.8 Å) distances, all of the hydrogen bonds can be categorized to be of a moderate strength (2.8–3.2 Å).³³ On the basis of the solid-state data, it can be of interest to examine the possible dimerization of **1_{syn}** in organic or aqueous solvents. Our preliminary data point to a monomeric form in CDCl₃ and likely dimeric in D₂O (10% DCl). The experimentally determined structure of **1_{syn}**, encompassing a dimer, is almost equivalent to its DFT energy-minimized form (Figure 6). In the X-ray resolved structure, one of the aromatic arms in **1_{syn}** is moved toward the bowl interior ($\Delta\alpha = 2.0^\circ$), while the other two are turned more distant ($\Delta\alpha = -0.27^\circ$). The molecule is

(23) The data collection crystal was a pale yellow rectangular rod with a pointed end. Examination of the diffraction pattern on a diffractometer indicated an orthorhombic crystal system. All work was done at 150 K, using a cryostream cooler. The data collection strategy was set up to measure an octant of reciprocal space with a redundancy factor of 3.6, which means that 90% of the reflections were measured at least 3.6 times. φ and ω scans with a frame width of 1.0° were used. Data integration, scaling, and merging were done computationally.²⁴ Merging the data and averaging the symmetry equivalent reflections resulted in an R_{int} value of 0.054. The structure was solved by the direct methods procedure.²⁵ Full-matrix least-squares refinements based on F^2 were performed computationally.^{26, 27} The asymmetric unit contains two of the bowl-shaped molecules, with each containing a crystallographic mirror plane, three water molecules, and some regions of disordered electron density. The solvents used for recrystallization were ethyl acetate and hexane, but neither of these molecules were recognizable in the disordered regions. The SQUEEZE procedure²⁸ of PLATON²⁹ was used to account for this disordered solvent. The total solvent accessible void is 1549 Å³, and the electron count for this region is 200 electrons/unit cell. The hydrogen atoms on the bowl-shaped molecules were included in the model at calculated positions by using a riding model with $U(\text{H}) = 1.2U_{\text{eq}}$ (attached atom). The hydrogen atoms of the water molecules were located on difference electron density maps and refined isotropically. All of these hydrogen atoms of the three water molecules are involved in an intermolecular hydrogen bonded network with the bowl-shaped molecules. The final refinement cycle was based on 8642 intensities and 460 variables and resulted in agreement factors of $R1(F) = 0.099$ and $wR2(F^2) = 0.175$. For the subset of data with $I > 2\sigma(I)$, the $R1(F)$ value is 0.058 for 5143 reflections. The final difference electron density map contains maximum and minimum peak heights of 0.29 and $-0.27 \text{ e}/\text{Å}^3$. Neutral atom scattering factors were used and include terms for anomalous dispersion.³⁰

(24) DENZO: Otwinowski, Z.; Minor, W. *Methods Enzymology*; Vol. 276, Macromolecular Crystallography, Part A; Carter, C. W., Jr., Sweet, R. M., Eds.; Academic Press: New York, 1997; pp 307–326.

(25) Sheldrick, G. M. *SHELXS-97*; Universitat Göttingen: Göttingen, Germany, 1997.

(26) Sheldrick, G. M. *SHELXL-97*; Universitat Göttingen: Göttingen, Germany, 1997.

(27) Farrugia, L. J. *J. Appl. Crystallogr.* **1999**, *32*, 837–838.

(28) Sluis, P. V. D.; Spek, A. L. *Acta Crystallogr.* **1990**, *A46*, 194.

(29) Spek, A. L. *Acta Crystallogr.* **1990**, *A46*, C34.

(30) *International Tables for Crystallography*; Kluwer Academic Publishers: Dordrecht, The Netherlands, 1992; Vol. C.

(31) (a) Hunter, C. A.; Sanders, J. K. M. *J. Am. Chem. Soc.* **1990**, *112*, 5525. (b) Cockroft, S. L.; Hunter, C. A.; Lawson, K. R.; Perkins, J.; Urch, C. J. *J. Am. Chem. Soc.* **2005**, *127*, 8594.

(32) The interior volume of **1_{syn}** was calculated following Rebek's protocol. See: Mecoski, S.; Rebek, J., Jr. *Chem. Eur. J.* **1998**, *37*, 3303.

(33) Jeffrey, A. G. *An Introduction to Hydrogen Bonding*; Oxford University Press, Inc.: New York, 1997; pp 11 and 12.

thus well preorganized to undergo the dimerization, and without considerable conformational adjustments fill its inner space in the solid state.

Conclusions

Transition metal-catalyzed transformations can be a subject of templation to boost the reaction stereoselectivity and maneuver the desired formation of covalent bonds. Here, we demonstrated a utility of template-directed synthesis for the preparation of a new family of bowl-shaped molecules. They comprise a semirigid frame and adjustable size cavity capable of coordinating transition metal cations. Studies of encapsulation and dynamic modulation of chemical reactivity with these reported hosts are in progress.

Experimental Section

Typical Procedure for the Synthesis of Compound 1. To a solution of **7** (0.050 g, 0.115 mmol) in anhydrous DMF (0.5 mL), at room temperature and under an atmosphere of argon, were added cesium fluoride (0.035 g, 0.230 mmol), copper(I) iodide (0.004 g, 0.023 mmol), and Pd(PPh₃)₄ (0.013 g, 0.0115 mmol). The reaction mixture was heated at 45 °C for 17 h. Diethyl ether (20 mL) and water (10 mL) were added successively, and the resulting solution was filtered under vacuum. The solid residue was washed with diethyl ether (50 mL) and ethyl acetate (50 mL), and the combined organic phase was dried (Na₂SO₄) and concentrated under reduced pressure. The resulting solid was purified by column chromatography (SiO₂, toluene/acetone, 3:1) to yield **1_{syn}** as gray (0.0043 g, 20%) and **1_{anti}** as orange solids (0.0033 g, 15%).

Data for Compound 1_{syn}. Mp > 430 °C; ¹H NMR (CDCl₃, 400 MHz) δ 7.78 (m, 6H), 7.42 (m, 6H), 4.86 (s, 6H), 2.96 (d, 3H, $J = 1.5$ Hz), and 2.85 (d, 3H, $J = 1.5$ Hz); ¹³C NMR (CDCl₃, 100 MHz) δ 163.2, 139.9, 138.8, 128.8, 128.6, 60.8, 49.3; HRMS(ESI) m/z calcd for C₃₉H₂₄N₆H 577.2140 [$M + H$]⁺, found 577.2144.

Data for Compound 1_{anti}. Mp > 430 °C; ¹H NMR (CDCl₃, 400 MHz) δ 8.02 (m, 2H), 7.94 (m, 2H), 7.87 (m, 2H), 7.70 (m, 2H), 7.56 (m, 4H), 4.68 (m, 6H), 2.80 (m, 5H), and 2.61 (d, 1H, $J = 9.4$ Hz); ¹³C NMR (CDCl₃, 100 MHz) δ 164.1, 163.8, 163.4, 139.9, 139.7, 139.3, 139.2, 139.1, 139.0, 129.2, 128.9, 128.9, 128.9, 128.6, 60.2, 60.1, 60.0, 49.3, 49.2; HRMS(ESI) m/z calcd for C₃₉H₂₄N₆H 577.2140 [$M + H$]⁺, found 577.2143.

Compound **1_{anti}** was proven difficult to purify with column chromatography. Therefore, to verify its quantity produced in a reaction, we used pentaerythritol tetrabromide as internal standard to reveal its concentration by ¹H NMR spectroscopy.

Compound 2.¹¹ To a solution of DMSO (4.0 mL) and CH₂Cl₂ (33.0 mL), at -78°C and under an atmosphere of argon, was added trifluoroacetic anhydride (10.73 g, 51.10 mmol) dropwise over a period of 1 h. Subsequently, bicyclo[2.2.1]hept-5-ene-2,3-diol¹¹ (2.26 g, 17.93 mmol) dissolved in CH₂Cl₂ (12 mL) was added over 10 min. The reaction mixture was allowed to stir at -78°C for 2 h, after which it was quenched with triethylamine (9.54 g, 94.31 mmol). The mixture was then left to stir for 3 h at ambient temperature, diluted with a solution of HCl (20 mL, 2.0 M), and extracted with CH₂Cl₂ (4 × 50 mL). The combined organic phase was dried (Na₂SO₄) and concentrated under reduced pressure to yield an orange oil. Pure **2** was obtained in a vacuum distillation (1.50 g, 60%). Bp 80 °C at 1.0 mm·Hg (lit.¹¹ bp 145 °C at 10.0 mm·Hg); ¹H NMR (CDCl₃, 400 MHz) δ 6.51 (m, 2H), 3.31 (m, 2H), 2.96 (d, 1H, $J = 10.8$ Hz), 2.49 (d, 1H, $J = 10.8$ Hz); ¹³C NMR (CDCl₃, 100 MHz) δ 195.6, 137.7, 51.4, 43.6.

Compound 4. To a solution of **2** (0.69 g, 5.65 mmol) in CH₂Cl₂ (25.0 mL) was added 1,2-phenylenediamine **3** (0.61 g, 5.65 mmol) over a period of 30 min. The reaction was allowed to stir for 1.5 h and then concentrated under reduced pressure. The resulting solid was purified by column chromatography (SiO₂,

toluene/acetone, 9:1) to afford **14** as a light-yellow solid (0.726 g, 66%). Mp 129 °C; ¹H NMR (CDCl₃, 400 MHz) δ 7.90 (m, 2H), 7.62 (m, 2H), 6.86 (s, 2H), 3.95 (s, 2H), 2.75 (d, 1H, *J* = 8.7 Hz), 2.57 (d, 1H, *J* = 8.7 Hz); ¹³C NMR (CDCl₃, 100 MHz) δ 166.4, 142.31, 139.2, 128.6, 128.6, 63.0, 49.6; HRMS(ESI) *m/z* calcd for C₁₃H₁₀N₂H 195.0922 [*M* + H]⁺, found 195.0921.

Compounds 5_{a/b}. To a *cis*-decaline (30.0 mL) solution of **4** (0.726 g, 3.74 mmol) at 150 °C was added a solution of bromine (0.776 g, 4.86 mmol) in *cis*-decaline slowly over 10 min. The mixture was stirred at the same temperature for 20 min, upon which the solvent was removed in vacuo. The residue was washed with acetone, filtered, and purified by column chromatography (SiO₂, hexanes/CH₂Cl₂, 1:4) to afford **5_a** and **5_b** as tan solids (1.18 g, 90%).

Data for Compound 5_a. Mp 148 °C; ¹H NMR (CDCl₃, 400 MHz) δ 8.03 (m, 2H), 7.74 (m, 2H), 4.39 (s, 2H), 3.91 (s, 2H), 2.97 (d, 1H, *J* = 10.8 Hz), 2.39 (d, 1H, *J* = 10.8 Hz); ¹³C NMR (CDCl₃, 100 MHz) δ 159.8, 142.0, 129.3, 55.7, 51.9, 41.9; HRMS(ESI) *m/z* calcd for C₁₃H₁₀Br₂N₂H 354.9264 [*M* + H]⁺, found 354.9263.

Data for Compound 5_b. Mp 139 °C; ¹H NMR (CDCl₃, 400 MHz) δ 8.11 (m, 1H), 8.04 (m, 1H), 7.74 (m, 2H), 4.84 (s, 1H), 4.12 (s, 1H), 3.84 (br, 1H), 3.81 (m, 1H), 2.76 (d, 1H, 10.9 Hz), 2.45 (d, 1H, *J* = 10.6 Hz); ¹³C NMR (CDCl₃, 100 MHz) δ 159.1, 158.9, 142.0, 141.7, 129.7, 129.6, 129.5, 129.2, 54.5, 54.3, 54.1, 52.5, 45.6; HRMS(ESI) *m/z* calcd for C₁₃H₁₀Br₂N₂H 354.9264 [*M* + H]⁺, found 354.9262.

Compound 6. To a solution of **5_{a/b}** (1.15 g, 3.26 mmol) in anhydrous THF (40 mL), cooled to 0 °C, was added potassium *tert*-butoxide (2.20 g, 19.5 mmol) portionwise. The reaction was allowed to stir for 2 h, quenched with water (5 mL), and subsequently extracted with diethyl ether (4 × 50 mL). The combined organic layer was dried (MgSO₄) and concentrated under reduced pressure. The resulting crude product was purified by column chromatography (SiO₂, toluene/acetone, 20:1) to afford **6** as a tan solid (0.825 g, 93%). Mp 111 °C; ¹H NMR (CDCl₃, 400 MHz) δ 7.94 (m, 1H), 7.92 (m, 1H), 7.65 (m, 2H), 6.87 (d, 1H, *J* = 3.3 Hz), 4.02 (m, 1H), 3.94 (m, 1H), 2.99 (m, 1H), 2.62 (m, 1H); ¹³C NMR (CDCl₃, 100 MHz) δ = 164.4, 164.2, 139.7, 139.3, 139.2, 134.9, 129.1, 129.0, 128.9, 128.7, 62.4, 57.4, 51.0; HRMS(ESI) *m/z* calcd for C₁₃H₉BrN₂H 273.0022 [*M* + H]⁺, found 273.0023.

Compound 7. To a solution of dry diisopropylamine (1.3 mL, 9.15 mmol) in dry THF (9.0 mL) at 0 °C was added *n*-butyllithium (5.7 mL, 1.6 M in hexane) under an atmosphere of argon. The reaction mixture was cooled to −78 °C, and a solution of **6** (0.500 g, 1.83 mmol) in THF (4.0 mL) was added dropwise over 10 min. The resulting mixture was stirred for an additional 30 min before a solution of trimethyltin chloride (0.44 g, 2.2 mmol) in THF (3.0 mL) was added. After 2 h at −78 °C, the reaction mixture was gradually warmed to room temperature, washed with water (15 mL), and extracted with diethyl ether (3 × 50 mL). The combined organic phase was dried (MgSO₄) and concentrated in vacuo. The solid residue was purified by column chromatography (SiO₂, toluene/acetone, 20:1) to afford **7** as an off-white solid (0.591 g, 75%). Mp 104–105 °C; ¹H NMR (CDCl₃, 400 MHz) δ 7.97 (m, 1H), 7.93 (m, 1H), 7.65 (m, 2H), 4.07 (dd, 1H, *J*₁ = 3.4 Hz, *J*₂ = 1.6 Hz), 3.94 (dd, 1H, *J* = 3.2 Hz, *J*₂ = 1.7 Hz), 2.92 (dt, 1H, *J*₁ = 8.8 Hz, *J*₂ = 1.7 Hz), 2.58 (dt, 1H, *J*₁ = 8.8 Hz, *J*₂ = 1.6 Hz), 0.27 (t, 9H, *J* = 27.6 Hz); ¹³C NMR (CDCl₃, 100 MHz) δ 164.9, 164.6, 153.9, 145.6, 139.6, 139.4, 129.0, 128.9, 128.8, 128.8, 61.9, 59.5, 56.3, −8.8; HRMS(ESI) *m/z* calcd for C₁₆H₁₇BrN₂SnH 436.9662 [*M* + H]⁺, found 436.9664.

Compound 8. To a solution of **7** (0.05 g, 0.115 mmol) in dry DMF (1.0 mL), heated to 70 °C, were added palladium(II) acetate (0.003 g, 0.011 mmol), triphenylphosphine (0.006 g, 0.023 mmol), and a trace amount of lithium chloride. The reaction was allowed to stir for a period of 1 h upon which additional portions (0.003 g, 0.011 mmol) of palladium(II) acetate were added, each at 3, 4, 5, and 20 h. The solvent was concentrated under reduced pressure and crude product was purified by column chromatography (SiO₂, toluene/acetone, 40:1) to afford **8** as a light-yellow solid (0.005 g, 19%). ¹H NMR (CDCl₃, 400 MHz) δ 7.90 (m, 2H), 7.60 (m, 2H), 3.61 (s, 2H), 2.66 (d, 1H, *J* = 8.6 Hz), 2.46 (d, 1H, *J*₁ = 9.4 Hz), 1.78 (s, 6H); ¹³C NMR (CDCl₃, 100 MHz) δ 166.7, 143.4, 139.2, 128.6, 128.3, 58.7, 54.4, 13.6; HRMS(ESI) *m/z* calcd for C₁₅H₁₄N₂H 223.1235 [*M* + H]⁺, found 223.1231.

Computational Details.³⁴All calculations for energy optimization of **1_{syn}** and its complexes [**1_{syn}**:Ag], [**1_{syn}**:Ag₂], [**1_{syn}**:Ag₃], and [**1_{syn}**:Cs:Cu₃] were completed with the Resolution of Identity Density Functional Theory (RI-DFT) method and by using formate ions attached to Ag(I) for charge neutralization.^{35–36} The Generalized Gradient Approximation (GGA) BP86 functional^{21b} was adopted. The RI-DFT method was used as implemented in TURBOMOLE.^{37–43} The triple- ζ plus polarization (TZVP) basis sets were used for the lighter elements, while for silver and cesium, relativistic effective core potential (ECP) and def-SV(P) basis sets were applied.⁴¹ Compounds **1_{syn}**, [**1_{syn}**:Ag₃], and [**1_{syn}**:Cs:Cu₃] were optimized with assumed C_{3v} symmetry. To compute the potential energy profile as a function of the N–N distance in **1_{syn}** (Figure S30, Supporting Information), the relaxed potential energy surface was scanned along the N–N trajectory (Table S12, Supporting Information).

Acknowledgment. We thank Professor Jon Parquette of the Ohio State University for useful suggestions. This work was financially supported with funds obtained from the Ohio State University, and the National Science Foundation under CHE-0716355.

Supporting Information Available: Additional experimental and computational results, and spectra for all new compounds. This material is available free of charge via the Internet at <http://pubs.acs.org>.

JO701538G

(34) For recent studies employing the BP86 functional in investigating organometallic systems, see: (a) Wang, F.; Li, L. M. *J. Comput. Chem.* **2004**, *25* (5), 669. (b) Silva, V. D.; Dias, R. P.; Rocha, W. R. *Chem. Phys. Lett.* **2007**, *439*, 69. (c) Nakamura, A.; Ohshima, T.; Mashima, K. *J. Organomet. Chem.* **2005**, *690*, 4373. For a recent comparison of DFT methods for organometallic systems, see: Furche, F.; Perdew, J. P. *J. Chem. Phys.* **2006**, *124*, 044013.

(35) Eichkorn, K.; Treutler, O.; Öhm, H.; Häser, M.; Ahlrichs, R. *Chem. Phys. Lett.* **1995**, *242*, 652.

(36) Eichkorn, K.; Weigend, F.; Treutler, O.; Ahlrichs, R. *Theor. Chem. Acc.* **1997**, *97*, 119.

(37) Becke, A. D. *Phys. Rev. A* **1988**, *38*, 3098.

(38) Schäfer, A.; Horn, H.; Ahlrichs, R. *J. Chem. Phys.* **1992**, *97*, 2571.

(39) Ahlrichs, R.; Bär, M.; Häser, M.; Horn, H.; Kolmel, C. *Chem. Phys. Lett.* **1989**, *162*, 165.

(40) Häser, M.; Ahlrichs, R. *J. Comput. Chem.* **1989**, *10*, 104.

(41) Von Arnim, M.; Ahlrichs, R. *J. Comput. Chem.* **1998**, *19*, 1746.

(42) Deglmann, P.; Furche, F.; Ahlrichs, R. *Chem. Phys. Lett.* **2002**, *362*, 511.

(43) The Turbomole basis set library is available via ftp from <ftp://ftp.chemie.uni-karlsruhe.de/pub/basen>.